

# GEOREFERENCING FROM GEOEYE-1 IMAGERY: EARLY INDICATIONS OF METRIC PERFORMANCE

C.S. Fraser & M. Ravanbakhsh

Cooperative Research Centre for Spatial Information, Department of Geomatics,  
The University of Melbourne VIC 3010, Australia - (c.fraser, m.ravanbakhsh)@unimelb.edu.au

**KEY WORDS:** GeoEye-1, RPCs, geopositioning, accuracy evaluation, bias compensation, satellite imagery

## ABSTRACT:

GeoEye-1 was launched in September 2008, and after some five months of commissioning commenced commercial operations in February, 2009. With its 0.41m panchromatic and 1.65m multispectral resolution, GeoEye-1 represents a further step along the way to higher resolution capabilities for remote sensing satellites. Given experiences with precise georeferencing from its sister satellite, IKONOS, initial accuracy expectations for 3D georeferencing with ground control entered the 20-40cm range, and geolocation utilising metadata (orbit and attitude recordings) alone is specified at 2-3m. This paper describes an early experimental assessment of the accuracy of georeferencing from GeoEye-1 imagery. A stereo panchromatic image pair covering the Hobart HRSI test field in Australia was utilised in the testing. This test field, originally established to support metric testing of IKONOS imagery, comprises more than 100 precisely measured GCPs, of which 55 were deemed suitable for the GeoEye-1 tests. Three aspects were investigated with the resampled 50 cm imagery: the first was the geolocation accuracy attainable from utilising vendor supplied RPCs, ie those generated utilising metadata alone; the second was the accuracy attainable via bias-corrected RPCs; and the third involved application of a linear empirical model, not so much to offer an alternative geopositioning capability, but more to gain an insight into the degree of linearity of GeoEye-1's east-to-west image scanning. The paper will highlight the fact that with bias-corrected RPCs and a single GCP, the RMS georeferencing accuracy reaches the unprecedented level of 0.10m (0.2 pixel) in planimetry and 0.25m (0.5 pixel) in height.

## 1. INTRODUCTION

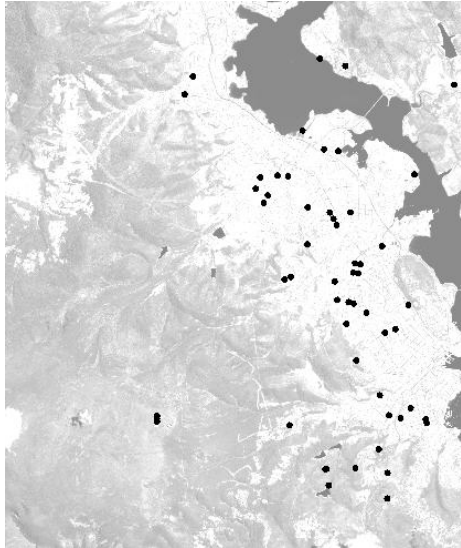
GeoEye-1, launched in September 2008, is the latest in a series of commercial high-resolution earth observation satellites. With its ground sample distance (GSD) of 0.41m for the panchromatic band, GeoEye-1 offers the highest resolution yet available to the spatial information industry. However, for commercial users, image products are down-sampled to 0.5m GSD. Specifications for GeoEye-1 quote a geolocation accuracy of better than 3m without ground control for mono and stereo image configurations, specifically 2m and 2.5m Circular Error 90% (CE90) in planimetry for stereo and mono, respectively, and 3m Linear Error 90% (LE90) in height for stereo coverage (GeoEye, 2009). GeoEye-1 will thus constitute a suitable source of imagery for large scale topographic mapping, to scales of 1:5,000 and possibly larger.

Following a 5-month commissioned phase, commercial operations with GeoEye-1 commenced in February, 2009. Not surprisingly, one of the first issues of interest within the photogrammetric community concerning GeoEye-1 has centred upon the system's potential for precise geopositioning and subsequent generation of digital elevation models (DEMs) and orthoimages. Based on nearly a decade of experience with imagery from IKONOS and other high-resolution satellite imaging (HRSI) systems, one could infer that geopositioning accuracy to around 0.5 to 0.7 pixels in planimetry and 0.7 to 1 pixel in height would be readily achievable from GeoEye-1 imagery. Moreover, for north-to-south scanning, accuracy in the along-track direction could be anticipated to be less than in the cross-track direction (Grodecki et al., 2003; Fraser et al., 2006). Application of vendor supplied rational function coefficients (RFCs) is assumed, with sensor orientation biases having been compensated through RPC-bias correction (Fraser & Hanley, 2003; Grodecki & Dial, 2003) via a modest number of high

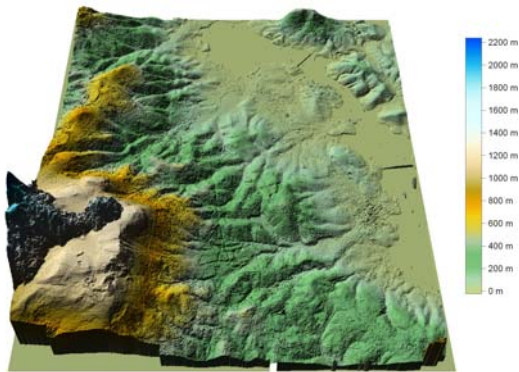
quality ground control points (GCPs), one being the minimum required. Also assumed is an image mensuration accuracy of better than 0.5 pixels, via manual measurement or image matching. For GeoEye-1, which has similar imaging characteristics to IKONOS (basically the same orbit height, but with a larger imaging scale as a consequence of a 13m focal length camera), these findings suggest an impressive georeferencing accuracy of around 0.25-0.3m in planimetry and, say, 0.4m in height from stereo imagery.

In mid-February, the authors were fortunate to be provided with a stereopair of GeoEye-1 images covering the Hobart HRSI test field (Fraser & Hanley, 2003; 2005). This test field covers an approximately 120km<sup>2</sup> area with topography varying from undulating terrain near sea-level to a mountain top at over 1200m elevation. Land cover varies from forest to suburbia, to the central business district of Hobart. Figure 1 shows both the GCP layout and a DEM for the test field. In the context of high-precision georeferencing from HRSI, a unique feature of the Hobart test field is that the majority of GCPs are road roundabouts, with the position of these having been determined through the computation of best-fit ellipses to a dozen or so points around the roundabout, measured in both object space and image space.

This paper will describe the process by which the geopositioning accuracy of GeoEye-1 was quantified, perhaps for the first time, within the Hobart test field. The account of this experimental assessment concentrates on practical aspects, in that current software systems, notably the *Barista* system (Barista, 2009), were used. As will be seen, the final results are very impressive. They illustrate that GeoEye-1 can yield geopositioning accuracy (RMS 1-sigma) of close to 0.10m (0.2 pixels) in planimetry and 0.25m (0.5 pixels) in height through the use of a single GCP.



(a) Geoeeye-1 scene showing final 55 GCPs



(b) IKONOS-derived DEM

Figure 1. Hobart HRSI Test Field.

## 2. IMAGE DATA SET AND TEST FIELD

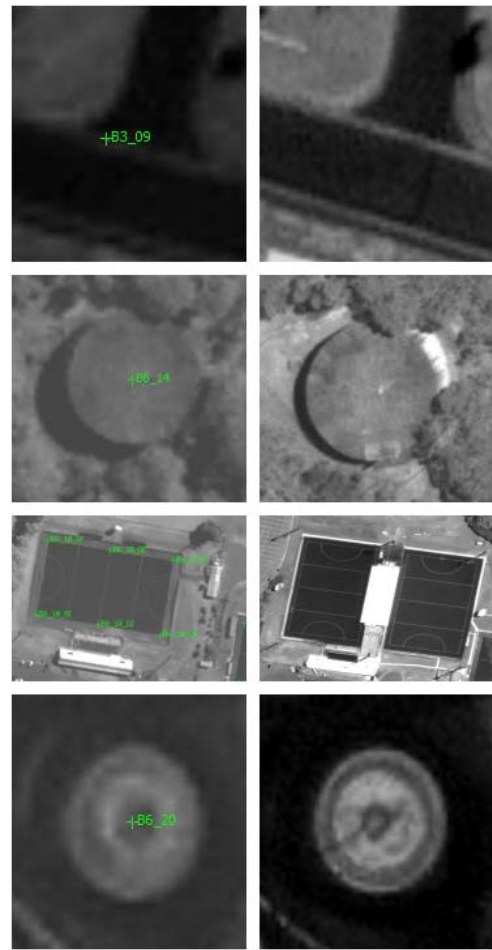
### 2.1 GeoEye-1 Stereopair

The GeoEye-1 stereo images were captured using a scanning azimuth of  $270^\circ$ , ie east-to-west, on 5 February 2009, with the panchromatic band and all four multispectral bands being recorded. The scene, shown in Figure 1, covered an area of 13.5km in the E-W direction by 15.8km N-S (the nominal scene width of GeoEye-1 is 15.2km). The forward looking image had a collection azimuth of  $53.4^\circ$  and an elevation of  $63.9^\circ$ , while the corresponding values for the backward looking image were  $139.7^\circ$  and  $70.1^\circ$ . This produced a Base/Height ratio of 0.6. Within the accuracy analysis described here, only the panchromatic band has been considered, with the images having been processed to standard geometrically corrected level, as well as bundle-adjusted without reference to GCPs prior to the generation of the RPCs.

### 2.2 GCP Array and Image Measurements

It had been 6 years since the GCPs of the Hobart test field were measured by GPS. Thus, the first stage of the accuracy evaluation process was to ascertain which GCPs still constituted good control. Initially, all GCPs were back projected into the stereo images and a visual assessment was undertaken. It

immediately became clear that many of the 100 or so original GCPs that fell within the GeoEye-1 scene area would not be usable. Some points had ‘moved’, for example markings on sports fields and tennis courts, hedge intersections and even some road detail; whereas others, while being sufficiently definable for IKONOS purposes, were insufficiently so for the 50cm resolution of GeoEye-1. Examples of ‘moved’ points both subtle and obvious, are shown in Figure 2. As a result of this initial assessment, some 65 GCPs were selected for image measurement, including three at 1260m elevation on the top of Mt Wellington, even though these fell a little short of the quality required. All but a dozen or so of the GCPs were road roundabouts.



(a) IKONOS (b) GeoEye-1

Figure 2. Examples of GCPs which had either ‘moved’ or were otherwise deemed unsuitable.

The image measurements were carried out via monoscopic digitisation within the *Barista* HRSI data processing system (Willneff et al., 2005; Barista, 2009), with two independent data sets being obtained. At least 10 points were digitised on the circumference of each roundabout, with the computed standard error of the centre point in the best-fitting ellipse computation being in the range of 0.04 to 0.08 pixels. In order to avoid the possibility of back-projected points biasing the image measurement process, the RPCs were manually altered such that existing GCPs, which served as guide points, were projected 10m below (south of) their true positions in the images. Smaller biases were present in the RPCs as well, which is a subject that we will now turn to.

### 3. IMPACT OF RPC BIASES

#### 3.1 Initial Determination via Monoplotting

Biases in HRSI RPCs generated from sensor orientation, which are generally attributed to small systematic errors in gyro and star tracker recordings, have been shown to be adequately modelled by zero-order shifts in image space. For moderately flat terrain and near nadir imagery, these biases can be quite easily quantified by simply computing planimetric coordinates in object space via the RPCs and comparing these to known ground coordinates. In the case of oblique imagery over mountainous terrain, however, the concept of monoplotting needs to be adopted in order to achieve pixel-level accuracy for bias error determination.

The *Barista* software system incorporates monoplotting functions, monoplotting being the familiar photogrammetric procedure that enables 3D feature extraction from single, oriented images when an underlying DEM is available (Willneff et al., 2005; Huang & Kwoh, 2008). In the case of Hobart, an IKONOS-derived DEM was available. The height accuracy of this had been shown to be around 3m for the road roundabouts (Poon et al., 2005). A dozen GCPs were monoplotting in order to gain an initial estimate of the planimetric geopositioning biases. The resulting values for Easting and Northing coordinates were 1.1m and 3.1m (2.2 and 6.2 pixels) for the forward-looking image and -0.6m and -2.2m (-1.2 and -4.4 pixels) for the backward-looking image, the standard deviation of each estimate being very close to 0.25m.

#### 3.2 3D Biases from Spatial Intersection

Biases within the RPCs also have a direct impact on 3D geopositioning from a stereo image pair. For the Hobart GeoEye-1 stereo pair, geolocation was performed via spatial intersection using the supplied RPCs. Systematic errors in object points of -2.1m in Easting, 0.5m in Northing and -7.6m in height resulted. (The vertical bias was reduced in a subsequent reprocessing of this early sample data by Geoeeye.) It is noteworthy that modest biases of a few pixels in each image can be manifest as much more significant errors in height determination. One very encouraging feature of the initial 3D ground point determination was that the standard deviation for the resulting coordinate errors in object space was 0.12m in planimetry and 0.25m in height, which suggested the capability of bias-free geopositioning to an accuracy of 0.25 pixels in the horizontal and 0.5 pixels in the vertical.

The monoplotting and RPC spatial intersection determinations of biases were illustrative of two aspects which had previously become familiar with other HRSI systems, namely that although relative positional accuracy at the sub-pixel level can be readily achieved in the absence of ground control, absolute geolocation to 1-pixel or better accuracy cannot be assured without the provision of GCPs. While it might be tempting to compare the geopositioning errors found in Hobart to the geolocation accuracy specifications for GeoEye-1, this is not really valid. Implicit in the specified 2-2.5m CE90 and 3m LE90 values for GeoEye-1 is the assumption that a sizable random sample of data is available. In this context, however, the sample size of the 60+ ground points in the Hobart Testfield is only 1, since the same systematic error applies to all measured coordinates. We now turn our attention to the accuracy potential of GeoEye-1 in the case where such positional bias errors can be readily compensated.

### 4. BIAS-COMPENSATED OBJECT POINT DETERMINATION

#### 4.1 Bias-Compensation Model

A practical means of modelling and subsequently compensating for the biases inherent in RPCs is through a block-adjustment approach introduced, independently, by Grodecki and Dial (2003) and Fraser and Hanley (2003). In this approach, the standard rational function equations that express scaled and normalised line and sample image coordinates ( $l, s$ ) as ratios of 3<sup>rd</sup> order polynomials in scaled and normalised object latitude, longitude and height ( $U, V, W$ ) are supplemented with additional parameters, as indicated in Equation 1.

$$\begin{aligned} l + A_0 + A_1 l + A_2 s &= \frac{Num_l(U, V, W)}{Den_l(U, V, W)} L_s + L_0 \\ s + B_0 + B_1 l + B_2 s &= \frac{Num_s(U, V, W)}{Den_s(U, V, W)} S_s + S_0 \end{aligned} \quad (1)$$

Here, the parameters  $A_i, B_i$  describe an affine distortion of the image. Three likely choices for 'additional parameter' sets for bias compensation are:

- i)  $A_0, A_1, \dots, B_2$ , which describes an affine transformation,
- ii)  $A_0, A_1, B_0, B_1$ , which models shift and drift for a N-S scan, or  $A_0, A_2, B_0, B_2$ , which models shift and drift for an E-W scan; and
- iii)  $A_0, B_0$ , which represent image coordinate translations.

Practical experience with IKONOS imagery has indicated that of the terms comprising the general affine additional parameter model, the only two of significance in stereo pair orientation, even for very high accuracy applications, are the shift terms  $A_0$  and  $B_0$  (Baltsavias et al., 2005; Fraser et al., 2006; Lehner et al., 2005). This finding suggests that within the few seconds needed to capture an image, the time-dependent errors in sensor exterior orientation are constant.

An additional benefit of restricting the image correction model to shift terms alone is that the estimated parameters  $A_0$  and  $B_0$  can be directly applied to correct the original RPCs, thus providing a very effective means of bias-compensation (Fraser & Hanley, 2003; 2005). Alternatives such as utilising the full affine image correction model or modelling the orientation biases in object space lead to the necessity of regenerating the RPCs, which is a less straightforward option than simple correction. Moreover, as soon as drift and affine coefficients are included in the bias compensation model, the geometric distribution and number of GCPs becomes a factor of significance, whereas for compensation by shift-terms alone only a single GCP is needed and its location within the scene has no bearing on the bias-compensation process.

Equation 1 can be formulated into a linear indirect model for bias-compensated object point determination. Since the process involves a least-squares adjustment of image coordinate observations and the estimation of exterior orientation, albeit indirectly, it has been termed a 'bundle adjustment', or indeed a block adjustment in cases where a number of images are included.

Free-net bundle adjustment is generally taken to mean the computation of relative orientation free of any shape constraints imposed by ground control. This can be approximated in RPC block adjustment by utilising GCPs with low apriori weights,

which are sufficient to remove, at least numerically, the singularity arising from the datum not being ‘fixed’. This approach offers the advantage of producing a best-fit to ground control of the relatively oriented network of images. Or, expressed another way, the adjustment will yield a solution which minimises the RMS errors at checkpoints (used as GCPs with low weight). Unfortunately, this approach to a free-net solution will inflate the standard errors of object point coordinates, since uncertainties in the datum assignment are manifest in the estimated covariance matrix of object point coordinates. The benefits of the method lie in quantifying overall geolocation accuracy (expressed by the RMSE values at checkpoints), rather than in analysing internal precision.

#### 4.2 Free-Net Bias Compensation

In order to achieve a ‘free-net’ solution for the Hobart GeoEye-1 bundle adjustment, all GCPs were assigned a priori standard errors of 5m (i.e. 10 pixels), whereas the initial standard errors for image coordinates generally ranged from 0.05 pixels for sharply defined roundabouts to 0.5 pixels for point features. The bias-compensation adjustment was then computed for the final 55 point network (initial block adjustment runs led to rejection of a further 10 GCPs based on their ‘movement’ or lack of quality), with the adoption of shift terms  $A_0$  and  $B_0$  alone. The results of the adjustment are summarised in Table 1.

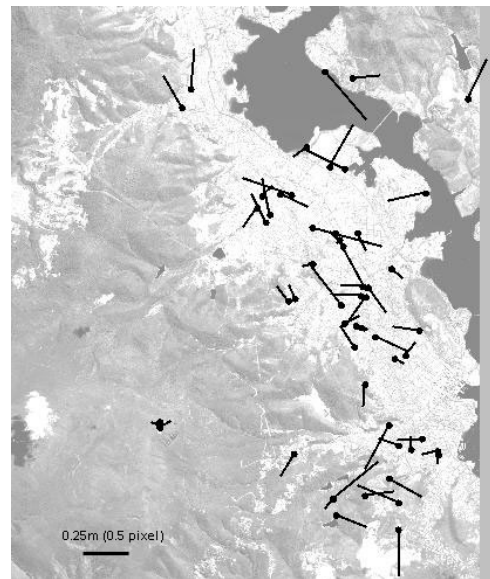
Foward-looking image	RMS of image residuals	Line (pixels)	Sample (pixels)
	Line/sample bias	6.7	-1.9
Backward-looking Image	RMS of image residuals	0.08	0.19
	Line/sample bias	-4.2	1.2
RMSE, 55 Chkpts	<u>Easting</u> <b>0.10</b> (m) (0.2 pixels)	<u>Northing</u> <b>0.10</b> (m) (0.2 pixels)	<u>Height</u> <b>0.18</b> (m) (0.4 pixels)
coordinate error range	-0.21 – 0.30m	-0.18 – 0.25m	-0.39 – 0.41m

Table 1. Results of 55-point free-net block adjustment with bias compensation.

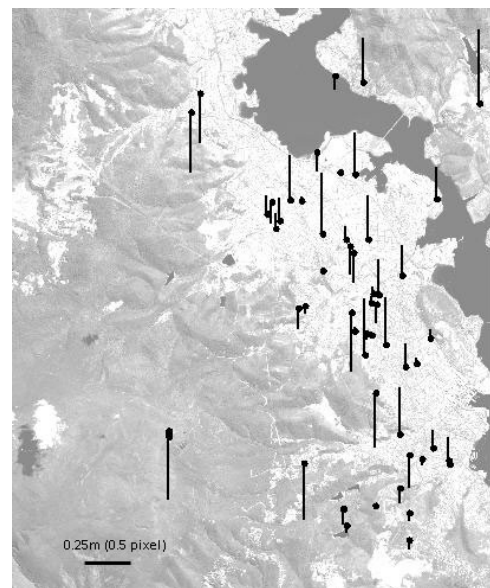
The most striking result presented in Table 1 is the very high accuracy achieved in geopositioning. The RMSE of geopositioning is at the unprecedented level of 0.2 pixels in planimetry and 0.4 pixels in height. This surpasses the results previously achieved with IKONOS or QuickBird by a significant amount and takes HRSI accuracy performance to a new level, at least in the authors’ experience. Whereas the anticipated discrepancy between RMS values of line and sample image coordinates is present, the line coordinates lying close to within the epipolar plane, the familiar difference between accuracy achieved in Northing versus Easting, which is normally associated with a N-S scanning direction, is no longer present, the scan here being E-W.

A cursory visual analysis of the checkpoint discrepancies in planimetry and height, shown in Figure 3, does not suggest the presence of unmodelled residual systematic errors. This would also suggest that the first-order bias compensation coefficients, in Equation 1 would not be significant. Additional bundle adjustment runs confirmed that this was indeed the case. Extending the image correction model to both shift and drift

parameters ( $A_0, A_2, B_0$  and  $B_2$ ), and the full affine model (all  $A_i$  and  $B_i$ ) did not alter the RMS value of image coordinate residuals by more than 0.02 pixels, or the RMSE values for object point coordinates by more than 0.02m.



(a) Planimetry



(b) Height

Figure 3. Check point discrepancies for the free-net block adjustment solution.

#### 4.3 Bias-Compensated Geopositioning from 1 or 2 GCPs

Given that under the free-net adjustment approach the relative orientation is free of shape constraints, the only distinction to be anticipated between the RMSE achieved when employing all checkpoints as GCPs of very low weight, versus employing one ‘fixed’ GCP and using the other 54 points as checkpoints alone, will arise from positional biases in the chosen GCP. Thus, if single GCPs are to be used for bias compensation, they should be as accurate in absolute terms as possible. In all other respects the relative orientation solutions should be the same, with the ‘fixed’ (zero variance) single GCP yielding valid estimates for the standard error of ground point determination.

For the Hobart GeoEye-1 stereo pair, two single-GCP bias-compensation adjustments were computed. In the first, the GCP was near the middle of the test field, at an elevation close to sea-level, and in the second the GCP was chosen to be one of the three points on Mt Wellington, at an elevation of 1260M. The results are summarised in Table 2. Not shown in the table are the values of the bias terms  $A_0$  and  $B_0$ , since these corresponded to the values listed in Table 1 to within 0.1 pixels for all adjustments. The computed standard errors for the shift parameters ranged from 0.15 pixels for the case of one GCP at sea level, to 0.1 pixel for the shift in the line coordinate for the single GCP on the mountain top. Also not shown in the figure are the RMS values of image coordinates, since these were in agreement to those in Table 1 to within 0.02 pixels.

1- or 2- GCP configuration	RMSE against 55 Checkpoints (m)			Mean Object Point Standard Error (m)		
	$s_E$	$s_N$	$s_H$	$\sigma_E$	$\sigma_N$	$\sigma_H$
Case A: 1 GCP at sea level	0.13	0.10	0.25	0.18	0.13	0.43
Case B: 1 GCP at 1260m elev.	0.11	0.10	0.28	0.19	0.13	0.45
2 GCPs from Case A & B	0.11	0.10	0.24	0.16	0.11	0.38

Table 2. Results of block adjustment with 1 and 2 GCPs.

One noteworthy aspect of Table 2 is that the checkpoint RMSE values are considerably smaller than is suggested by the corresponding coordinate standard errors, at least for the Easting coordinates and in height. For all practical purposes, the accuracies obtained match those achieved in the free-net approach, though there was the introduction of a small affinity in the height direction in the bias-compensation adjustments of Table 2. The causes of this small height error, which amounted to almost 2 pixels for the three points on Mt Wellington, is still to be fully ascertained. Its net effect was to inflate the overall RMSE values in height by 0.05 pixels to 0.5 pixels.

## 5. GEOPOSITIONING VIA AN EMPIRICAL MODEL

With the ready availability nowadays of either RPCs or comprehensive orbit and attitude metadata for commercial HRSI systems, there is generally little need to resort to empirical functions to describe the image to object space transformation. Nevertheless, the simplicity of models such as the 8-parameter 3D affine model is attractive. Also, application of such a first-order transformation function can provide insight into the ‘linearity’ of the scanning geometry throughout the scene. Partially for this reason, the affine model was applied to the Hobart GeoEye-1 stereo pair, again in free-net mode, with all 55 GCPs having an assigned priori standard error of two pixels. The resulting RMS value of image coordinates was 0.18 pixels for the forward-looking image and 0.14 pixels for the backward, with the values being similar in line and sample.

The RMSE values at the 55 checkpoints amounted to 0.3m in Easting, 0.8m in Northing and 0.2 in Height. In plotting the image coordinate residuals, as shown in Figure 4, a clear higher-order systematic error trend in the satellite track direction can be seen. This also exhibits a height dependence, in accordance with expectations (Fraser & Yamakawa, 2004).

The simple observation to make here is that the higher-order error signal is well accounted for by the 3<sup>rd</sup> order RPCs, but not by a first-order affine model. Nevertheless, the affine model produces geopositioning results of modest accuracy. It is suggested that the systematic nature of the residuals in Figure 4 should be a sufficient reason to adopt the bias-compensated RPC model whenever possible.

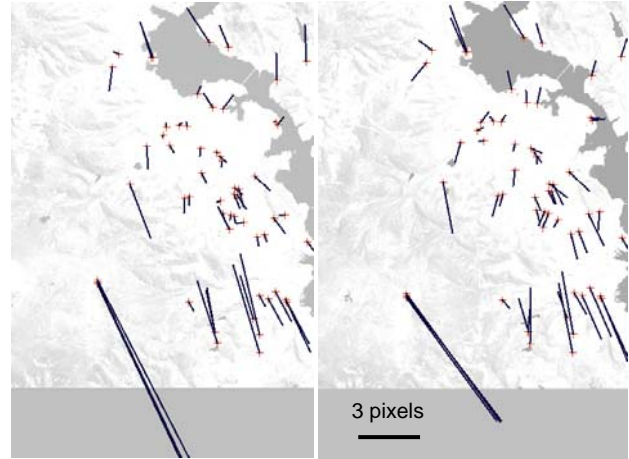


Figure 4. Image coordinate residuals from the 3D affine model.

## 6. CONCLUSIONS

This early investigation into the metric potential of GeoEye-1 stereo imagery has demonstrated that this new 0.5m resolution satellite imaging system is capable of producing unprecedented levels of ground point determination accuracy. With bias-compensation adjustment of the supplied RPCs, using an additional parameter model comprising two shift parameters only, geopositioning accuracy of 0.1m (0.2 pixels) in planimetry and 0.25m (0.5 pixel) in height can be attained with a single GCP. This level of metric performance surpasses design expectations, as indicated through standard error estimates, and it augurs well for the generation of both digital surface models to around 1-2m height accuracy and 0.25m GSD orthoimagery to sub-metre accuracy.

## ACKNOWLEDGEMENTS

The authors express their gratitude to Geoeeye for making the GeoEye-1 imagery available.

## REFERENCES

- Baltsavias, E., Li, Z., Eisenbeiss, H., 2005. DSM generation and interior orientation determination of Ikonos images using a testfield in Switzerland. *Int. Arch. Photogramm., Remote Sens. & Spatial Inf. Sc.*, Vol. 36, Part I/W3, 9 pages (on CD-ROM).
- Barista, 2009. <http://www.baristasoftware.com.au> (accessed 20 Mar. 2009)
- Fraser, C., Hanley H.B., 2003. Bias compensation in rational functions for IKONOS satellite imagery. *PERS*, 69(1): 53-57.
- Fraser, C.S., Hanley, H.B., 2005. Bias-Compensated RPCs for Sensor Orientation of High-Resolution Satellite Imagery. *PERS*, 71(8): 909-915.

- Fraser, C.S. and Yamakawa, T., 2004. Insights into the Affine Model for Satellite Sensor Orientation. *ISPRS J. of Photogramm. & Rem. Sens.*, 58(5-6): 275-288.
- Fraser, C.S., Dial, G., Grodecki, J., 2006. Sensor Orientation via RPCs. *ISPRS J. Photogramm. & Rem. Sens.*, 60: 182-194.
- GeoEye, 2009. GeoEye-1 web site: <http://launch.geoeye.com/LaunchSite/about/Default.aspx> (accessed 20 Mar. 2009)
- Grodecki, J., Dial, G., 2003. Block adjustment of high-resolution satellite images described by rational functions. *PERS*, 69(1), 59-68.
- Grodecki, J., Dial, G., Lutes, J., 2003. Error propagation in block adjustment of high-resolution satellite images. *Proc. ASPRS Annual Mtg*, Anchorage, 5-9 May, 10p. (on CD-ROM).
- Huang, X., Kwoh, L.K., 2008. Monoplotting – A semi-automated approach for 3D reconstruction from single satellite images. *Int. Arch. Photogramm., Rem. Sens. & Spatial Inf. Sc.*, 37(B3b-2): 735-740.
- Lehner, M., Mueller, R., Reinartz, P., 2005. DSM and Orthoimages from Quickbird and Ikonos data using rational polynomial functions. *Int. Arch. Photogramm., Rem. Sens. & Spatial Inf. Sc.*, 36 (I/W3), 6 pages (on CD-ROM).
- Poon, J., Fraser, C.S., Zhang, C., Zhang, L., Gruen, A., 2005. Quality Assessment of Digital Surface Models Generated from IKONOS Imagery. *Photogramm. Record*, 20 (110): 162-171.
- Willneff, J., Poon, J., Fraser, C.S., 2005. Monoplotting Applied to High-Resolution Satellite Imagery. *Journal of Spatial Science*, 50(2):1-11.